HHS Public Access

Author manuscript

Clin Exp Ophthalmol. Author manuscript; available in PMC 2018 July 18.

Published in final edited form as:

Clin Exp Ophthalmol. 2018 March ; 46(2): 158–168. doi:10.1111/ceo.13064.

Structural and Functional Imaging of Aqueous Humor Outflow

Alex S. Huang[1,2], **Brian A Francis**[1,2], and **Robert N. Weinreb**[3]

[1]Doheny Eye Institute, Los Angeles, CA

[2]Doheny Eye Centers, Los Angeles, CA; Department of Ophthalmology, David Geffen School of Medicine at University of California, Los Angeles

[3]Shiley Eye Institute and Hamilton Glaucoma Center, Department of Ophthalmology, University of California, San Diego

Abstract

Maintaining healthy aqueous humor outflow (AHO) is important for intraocular cellular health and stable vision. Impairment of AHO can lead to increased intraocular pressure, optic nerve damage, and concomitant glaucoma. An improved understanding of AHO will lead to improved glaucoma surgeries that enhance native AHO as well as facilitate the development of AHO-targeted pharmaceuticals. Recent AHO imaging has evolved to live human assessment and has focused on the structural evaluation of AHO pathways and the functional documentation of fluid flow. Structural AHO evaluation is predominantly driven by optical coherence tomography, and functional evaluation of flow is performed using various methods, including aqueous angiography. Advances in structural and functional evaluation of AHO are reviewed with discussion of strengths, weaknesses, and potential future directions.

Anatomy, Discovery, and History

Aqueous humor is produced by the ciliary processes of the eye and fills the sulcus (space behind iris and in front of the lens/zonule diaphragm) and anterior chamber spaces. Aqueous humor has several purposes including to provide essential biomolecules like electrolytes, micro-molecules, glucose and vitamin co-factors to intraocular tissues[1]. Aqueous humor flow also helps remove cellular waste. As related to vision, the presence of aqueous humor is critical to maintain a relatively stable intraocular pressure (IOP) for ocular rigidity, important for predictable optics.

IOP is determined by the balance of aqueous humor inflow and outflow (AHO).[2] Impaired AHO causes an increase in IOP, and this may lead to glaucoma as a result of optic nerve injury[3]. Two AHO pathways exist named the conventional (trabecular) and unconventional (uveoscleral) outflow pathways (Fig. 1).

Corresponding Author: Alex Huang, MD/PhD, Doheny Eye Institute, Department of Ophthalmology, David Geffen School of Medicine, University of California, Los Angeles, 1355 San Pablo Street, Los Angeles, CA 90033, Ahuang@Doheny.org, Phone: 323-442-6436; Fax: 323-442-6688.

Conventional (Trabecular) AHO

An early clue that intraocular fluid exited the eye came from Lauber's dog[4]. When comparing the hematocrit between peripheral veins in the extremities to that of ocular ciliary veins, higher hematocrit was observed in peripheral veins. Two hypothesis could have explained this phenomenon with the eye either actively extracting red blood cells from the blood or the eye exuding a clear fluid into the circulation. The latter was eventually proven to be true and found to be the result of the conventional (trabecular) outflow pathway. This pathway starts with aqueous in the anterior chamber (AC) passing through a multi-layered trabecular meshwork (TM)[3] and entering Schlemm's canal (SC; that lies along the limbus). Aqueous then moves through collector channels (CCs), into an intrascleral venous plexus, and eventually leading to aqueous and episcleral veins where the aqueous joins the venous circulation ultimately flowing to the right side of the heart[5, 6].

Unconventional (Uveoscleral) AHO

After conventional outflow was found as the first drain for fluid to exit the eye, uveoscleral outflow was identified as a second drain. In the mid-20th century, Anders Bill injected radiolabeled albumin into the eyes of various species. Collecting back conventional (trabecular) outflow on the surface of the eye (from severed episcleral veins), Bill wasn't able to recover a significant portion of the initially introduced radioactivity[7]. Performing autoradiography on sections cut from enucleated test eyes, the missing fraction was discovered to reside in the uvea and sclera leading to the designation of a new uveoscleral outflow pathway[8, 9]. Subsequent work delineated this pathway as aqueous moving into the ciliary body from the anterior chamber into ciliary body clefts and through the suprachoroidal space either exiting the eye via this vasculature or into/through the sclera[10]. More recently, an alternative lymphatic destination has been discovered as a variant of the uveoscleral pathway termed the uveo-lymphatic pathway[11].

Since imaging of uveoscleral outflow is more challenging, this review will focus on imaging of conventional (trabecular) outflow heretofore designated as trabecular, conventional, or simply aqueous humor outflow (AHO).

Structural Assessments of Conventional Aqueous Humor Outflow (AHO)

Early work on the structural anatomy of AHO pathways did not reflect its dynamic nature. Casting agents were injected into the eye, allowed to polymerize, and then after removal or digestion of ocular tissue, a three-dimensional (3D) representation was left[12, 13]. The disadvantage of casting studies was the need for firm (supraphysiologic) pressure to deliver the agent and the potential to create artifactual anatomy. Additionally, only static representations could be obtained, and dynamic changes (physiologic or pathologic) in outflow pathways could not be appreciated. Subsequently, further anatomical characterization relied on gross anatomy, histology, and electron microscopy[14, 15]. More recently, modern non-invasive tools exist to better describe the structural nature of AHO pathways. 3D micro-CT identified AHO pathways lumens given low radiographic signal and also allowed for 3D reconstruction, albeit in enucleated post-mortem eyes[16].

Today, the most widely-employed non-invasive structural assessment tool is vision science and ophthalmology is optical coherence tomography (OCT)[17]. OCT can be performed in live subjects and allows for longitudinal study. Initially developed for evaluating retinal structure and subsequently for optic nerve evaluation in both glaucoma diagnosis and treatment, OCT for trabecular AHO pathways is less mature. However, using anterior segment OCT (AS-OCT), initial outflow pathway structures such as TM, SC, and CCs have been imaged.

The TM has been reported to be imaged by AS-OCT. It is bounded medially by the anterior chamber, laterally by an arc-like hypodensity (interface shadow)[18], superiorly by Schwalbe's line and inferiorly by the scleral spur. TM measurements have been made in a wide variety of subjects across different ages and ethnicities[19–21]. Phase-based OCT (ph-OCT) has shown pulse-dependent TM motion in enucleated non-human primate[22] and live human eyes[23]. Simultaneously imaged with digital pulse-oximetry, this pulsatile motion synchronized with the digital pulse (albeit with a temporal offset), implying a cardiac origin[23].

A key limitation in TM imaging is that, while properly positioned, the ground-truth identity of the OCT signal in the angle including the arc-like hypodensity (interface shadow) has not been firmly established. Even with posterior-segment OCT, where there is a greater abundance of data and research, the labeling and histological identity of the various hypo- and hyper-reflective retinal bands have evolved over time with ever improving ground-truth and histological confirmation of OCT signal[24]. Therefore, the same needs to be done for the TM in the anterior segment. One proposed study could be to perform clinical canaloplasty on enucleated post-mortem human eyes. In canaloplasty, SC is exposed, and a fiberoptic probe is inserted and used as a guide to thread a suture throughout SC. Properly placed, the suture could serve as a fiducial point for multi-modal image comparison. The suture could be identified on OCT in relation to the arc-like hypodensity and then further identified in histological section in relation to SC and TM, with a comparison in between.

Compared to TM, SC study by AS-OCT is more established with a larger literature. The reason for this is that the fluid-filled SC lumen gives clear OCT hypo-reflective signal such that it can be easily identified, not unlike blood vessels. This has been done in post-mortem human eyes[25] and live eyes in small segments of normal[26, 27] and glaucomatous[18] individuals. Automated segmentation methods for SC using AS-OCT images have been created[28] (Fig. 2). Extrapolation of SC 360-degrees around the limbus into a three-dimensional representation has been done showing segmental anatomy with wider or narrower regions[28] (Fig. 3). In various species, pilocarpine[29], rho-kinase (ROCK) inhibitors[30], and laser trabeculoplasty[31] have been reported to increase the size of SC. In contrast, IOP elevation[32] has been shown to do the opposite.

Directly posterior to SC, CC identification by AS-OCT has been performed as well, also with automated segmentation (Fig. 2)[28]. However, OCT study of SC and CCs created a new challenge: how does one define a CC relative to SC on AS-OCT? For example, if looking for an OCT hyporeflective lumen, how could one distinguish an CC posterior and in-line with SC from an extra-long SC? Separately, since the interface shadow is hypothesized to contribute to the TM and also has low OCT signal, this shadow could be confused for CCs

by automated segmentation. To address this, characteristic-based definitions of CCs were required to help guide segmentation[28]. For example, characteristics included the position or angle at which CCs were positioned relative to SC. The downside of making definitions was that atypical CCs could be missed. For example, based on electron microscopic study[33], CCs can have different subtypes or configurations (standard circular or atypical complex). Furthermore, CCs could not only take complex and tortuous routes lending them to be missed by AS-OCT segmentation, but CC size and number could also dynamically change[34], making overall assessment even harder.

Compared to OCT in the posterior segment of the eye, additional challenges arise for AS-OCT evaluation of AHO pathways. First, the distance traveled is large. Unlike the macula, where clinical OCT imaging covers ~ 5–6 mm, comprehensive AS-OCT imaging of AHO structures must cover the entire circumference of the limbus (2 X π X radius [average 11.5 mm] = 36.11 mm). In one study, over 5000 B-scans were taken in overlapping volumes with high density to limit missing CCs[28]. This is compared to retina OCT where 50–100 scans can guide surgical decisions. Structures such as CC are also small. Typical commercial OCTs have a B-scan to B-scan distance of ~35 microns and can miss CCs. Ground-truth identification of AS-OCT hyper- and hypo-reflective structures are not definite as mentioned above. Posterior to the angle, identification of outflow pathways distal to SC and CC simply based on low OCT signal is complicated by the presence of other hyporeflective lumens not involved in AHO such as arteries, lymphatics, and some veins. Most importantly, unlike posterior-segment OCT which has tracking and reference functions that allow imaging of the same retina location longitudinally over time[35], in AS-OCT these abilities are lacking. It becomes difficult for investigators to know if AHO pathway imaging across two sessions are really in the same location and more importantly if at the same angle. All it takes is a shift in the image acquisition angle to make a single SC appear bigger of smaller across different image acquisition periods.

Finally, unlike the posterior segment where the structure:function (ganglion cell:visual field or OCT:visual field) relationship is well-studied[36–38], in the anterior segment, the relationship of AHO structure to fluid flow is unclear. For example, does a larger outflow lumen always equate to greater aqueous flow? Alternatively, could a big lumen represent trapping of stagnant fluid in an outflow cul-du-sac. Therefore, while AS-OCT imaging of AHO pathways has the enormous advantage of being non-invasive, in the future, significantly more AS-OCT research on AHO structural mapping with technological advances are needed. In the meantime, functional assessment of fluid flow may have a bigger role.

Functional Assessments of Conventional Aqueous Humor Outflow (AHO)

To complement structural data, functional AHO imaging involves visualizing where the fluid actually flows. Methods can be broken down into non-invasive versus invasive and static versus real-time. For imaging conventional AHO, only invasive methods, either static or real-time, exist.

In static AHO imaging, tracers are delivered into the anterior chamber for a set amount of time[39–47]. Then, the eye is prepared for microscopic or histological analyses regarding where the tracer has moved. Variables can include the amount of time that the tracer is allowed to flow in addition to tracer characteristics such as size.

Static AHO imaging has mostly involved gold particles, fluorescent microspheres ranging from 0.2–20 microns in size, or 0.01-micron quantum dots[39–47]. The molecular weight of water (which comprises the vast majority of aqueous humor) is 18 g/mol or daltons. Spheres and dots (consider the number of carbon molecules) can have molecular weight from 10^3–10^7 daltons so that these studies theoretically best model larger particulate movement. Because of this, tracers can accumulate at filtration points, and static AHO imaging has been quite useful in visualizing flow at the TM or CCs.

Static methods first demonstrated segmental patterns of TM uptake and encouraged the idea of segmental AHO. Early worked focused on post-mortem bovine and human eyes, often using isolated anterior segmental organ culture. After tracer introduction, TM utilization was quantified by calculating percent filtration length (PEFL)[39]. PEFL was determined in histological section by dividing the total distance or length (L) over which tracer was seen by the total length (TL) of outflow pathways observed (PEFL = L/TL).

Static methods demonstrating segmental AHO have also been used to learn about TM/SC biology. ROCK inhibitors abolished segmentalization seen through gold particle distribution viewed by electron microscopic analyses of SC cells[41]. In fluorescent microbead studies, ROCK inhibitors showed increase PEFL[48] while increasing IOP decreased PEFL[49]. Using mouse genetics, segmental TM AHO, seen in wild-type mouse, became more homogenous in a secreted protein acidic and rich in cysteine (SPARC) mutant[40]. To probe the underlying biology of high and low flow regions, said regions were also identified by microbead accumulation and isolated to enrich for biological differences. An increase in versican (a large extracellular matrix proteoglycan) was seen at the RNA and protein level in low flow human TM[47]. Alternatively, gene expression analysis with some immunofluorescence confirmation revealed increases in collagen and matrix metalloproteinases in high flow regions[46]. At the electron microscopic level, micron-sized pores (I-pores: intracellular pores for fluid flow across a cell; B-pores: border pores for paracellular flow between cells) have been hypothesized to move fluid past the contiguous border between the inner-wall of SC and juxtacanalicular TM[45]. Segmental tracer accumulation positively correlated with total pore and B-pore density suggesting that the paracellular pores represented the dominant pathway for transendothelial filtration across the SC inner-wall[45].

While static methods have revealed multiple insights about AHO biology, the key limitation was that they were not compatible with live human imaging. Safety of tracer particles have not been thoroughly investigated in live humans. Histological study, the most common analysis endpoint, is not possible in patients. Therefore, real-time imaging that avoids the need to process tissue for analyses is required. Episcleral venous fluid waves, canalograms and aqueous angiography represent three forms of invasive real-time AHO imaging.

Episcleral venous fluid waves were first described in the operating room[50]. Using conventional irrigation from phacoemulsification units during cataract surgery, it was noted that some post-limbal episcleral veins could disappear. This indicated forward flow of clear perfusate. When studied clinically and retrospectively, a statistically significant correlation was seen between patients with observable episcleral fluid waves and better surgical success using trabecular ablation[51]. The clear advantage of the episcleral venous fluid wave method was that it was an imaging technique designed with clinical instruments for the spirit of being compatible for humans.

However, a few limitations exist for episcleral venous fluid wave. First, the pressure is high. Intraocular pressure during phacoemulsification is difficult to accurately assess. While the height of the bottle reservoir is known so that the gravity-driven fluid pressure can be calculated, leaks around wounds are unquantifiable. Tactile pressure of the eye during phacoemulsification ultimately confirm what all cataract surgeons know, IOP is transiently high during surgery. While this is excellent for chamber stability and keeping the posterior capsule away from the phacoemulsification tip, high pressure also alters AHO, potentially collapsing portions of SC leading to non-physiologic results. Also, loss-of-signal methods (from the perfusate flushing the blood out) are more difficult to analyze compared to gain-of-signal methods. Loss-of-signal imaging requires surgeons to record, know, and remember the episcleral venous pattern before the perfusate is pushed forward in order to identify what was lost. Familiar to glaucoma specialists, this is the exact challenge of posterior segment OCT analysis of retinal nerve fiber layer (RNFL) loss. Normal RNFL databases with statistics are helpful comparators because, without patient-specific longitudinal exams or data, clinicians don’t know how much RNFL was “lost” at any particular time in any particular patient. This is compared to retinal OCT where, for example, the simple presence of intraretinal cysts are obviously pathologic without necessarily needing a database regarding normal retinal thicknesses. Thus, gain-of-signal imaging are usually preferable to loss-of-signal imaging.

Like the episcleral venous wave, canalography was another AHO imaging method that started with clinical surgeries, in this case canaloplasty. Canaloplasty was described above in the structural analyses of conventional (trabecular) AHO. In canalograms, after SC exposure, tracers could either be directly injected into SC with image acquisition in live subjects or during the reversal step when the canaloplasty probe was backed out of the eye to suture thread SC[52–55]. While backing out, dollops of tracer (normally viscoelastic to achieve a viscodilation) could be dropped to visualize AHO pathways.

Canalograms yielded excellent images showing outflow around the limbus[52–55]. However, by introducing the tracer into SC, the contribution of TM to outflow was not included, and this was not physiologic. Also, segmentalization was harder to appreciate. This was so because in order to assess segmental AHO, tracer must fairly reach all portions of the circumferential limbus at about the same time. If injecting directly into SC, local areas around the point of SC exposure automatically received tracer first and could appear to have more AHO than the opposite side of the eye. Even during the canaloplasty reversal step, it took time to back the probe circumferentially around the limbus out of SC. Therefore, a more circular wave of tracer delivery occurred peri-limbal as opposed to simultaneous.

To complement canalograms, aqueous angiography was devised. Aqueous angiography was also developed with the principle of starting with clinical (Spectralis HRA+OCT [Heidelberg Engineering, Heidelberg, Germany], indocyanine green [ICG], fluorescein etc…) and operating room (anterior chamber maintainer, tubing etc…) instrumentation for easier translation to patients. Bringing these supplies into the laboratory, aqueous angiography was first tested with post-mortem pig, cow, and human eyes[56–59]. Given that the Spectralis was a clinical instrument meant for adult humans with chins, enucleated eyes were secured to drilled holes in the eyes of Styrofoam heads commonly used in cosmetology schools because the models had chins.

To perform aqueous angiography, anterior chamber maintainers were inserted into the AC because, compared with standard needles, the grooved ridges lessened leakage at the entry point and prevented sliding. Constant-pressure gravity-driven tracer delivery was established from a reservoir placed over the eye for 10 and 20 mm Hg in experiments studying enucleated[56, 58, 59] and intact eyes of living subjects[60, 61], respectively. The images were taken with the angiographic function of the Spectralis (HRA+OCT) on fluorescein (excitation wavelength= 486 nm and transmission filter set at > 500 nm) or ICG (excitation wavelength= 786 nm and transmission filter set at > 800 nm) capture mode after establishing a dark pre-tracer background. To study segmental patterns, axial images were collected in post-mortem eyes. While axial imaging could slightly distort angiographic flow images due to normal globe curvature, only axial imaging allowed all quadrants of the eye to be simultaneously visualized for comparison. Since the eyelids blocked the post-limbal view in in living subjects, tractions sutures were required to rotate the eye in non-human primates[60]. In live humans[61], the subjects were instructed to move their eyes on their own.

Angiographic images were readily obtained, and multi-model imaging was used to validate angiographic signal as AHO. First, AS-OCT performed on (but not off) angiographic structures corresponded with intrascleral lumens that were consistent with AHO pathways[56–61]. Second, fixable fluorescent tracers that could be trapped were present to a much greater extent in TM associated with angiographically positive compared to negative regions[56–59]. Lastly, in intact eyes of living subjects, some of the observable episcleral veins overlapped with angiographic structures as would be expected for AHO[60, 61].

Segmental AHO was observed in all species (post-mortem: pig, cow, and human; intact/live: non-human primate and human). Divided into quadrants, quantification of angiographic intensity in pig eyes did not show a predilection to any quadrant[56]. In non-human primates and humans, nasal signal was predominantly seen post-mortem[59] and live[60, 61].

Potential clinical relevance for aqueous angiography was established using Minimally Invasive Glaucoma Surgeries (MIGS). MIGS are a new category of glaucoma surgery well-known for their ease, speed of surgery, and low risk profile. The most common MIGS are the trabecular-type where the TM is either ablated or bypassed. While successful in lowering IOP[62, 63], MIGS show some inconsistency. One hypothesis for this may be that the surgery has to be placed in the correct location. Normally, MIGS are placed in the nasal angle from a temporal approach. Some of the original arguments for this direction were based on previous literature showing more AHO pathways in the nasal portion of the eye[64]. However,

practicalities related to surgeon familiarity with the temporal approach (at least for cataract surgeons) also likely drove some of these initial recommendations.

With this in mind, one could ask whether trabecular MIGS should target higher or lower flow regions. For areas of high flow, placing a surgery there may allow access to known AHO pathways. However, if a quadrant has good AHO, it may be that the local TM already offers low resistance such that circumventing the TM may have minimal effect. In other words, there may be a ceiling that limits how much outflow improvement can occur. Alternatively, placing trabecular MIGS in regions of low flow may give more room for enhancement. However, it may be that regions of low flow were initially such because the anatomy for AHO was insufficient or incomplete.

Therefore, aqueous angiography was used to test whether low flow regions could be improved or rescued. First, using cow eyes, a two-dye system was devised where ICG aqueous angiography was performed followed by fluorescein aqueous angiography in the same eye[58]. This was comparable to laboratory set-ups using fluorescein and commonly found red fluorescent tracers[49, 65]. Patterns between ICG and fluorescein were sufficiently similar such that one could performed angiography with one dye, perform a hypothetical intervention (surgeries, lasers, or drugs), and then query the effect with the second dye.

With this in place, aqueous angiography-mediated guidance of trabecular bypass stents was performed[59]. ICG aqueous angiography was performed on post-mortem human eyes, and this was followed by sham touch or placement of a trabecular bypass stent in regions of initially low angiographic signal followed by fluorescein aqueous angiography. Not only was there rescue of angiographic signal comparing stent placement to control, but examples of partial TM bypass showed intermediate results[59]. AS-OCT imaging after TM stenting also showed successful movement of particulate matter into AHO pathways despite directing stent placement to initially low flow areas. Therefore, at least in post-mortem eyes, regions of low flow could be rescued[59]. However, greater study from intact eyes of living subjects was necessary.

To image intact eyes of living subjects, a different setup was necessary. Non-human primates and humans take supine positions in the operating room. Therefore, the Spectralis FLEX module (Heidelberg Engineering, Germany) was created (Fig. 4). The FLEX module was a modified surgical boom arm onto which a fully functional Spectralis HRA+OCT (identical to the table-mounted version in outpatient ophthalmology clinics) was installed. Multiple pivot joints allowed for multi-positional imaging including seated, tilted, lateral decubitus, supine, and even prone positions.

Studying intact eyes of living non-human primates and humans, segmental angiographic patterns were first confirmed[60, 61] (Fig. 5). Then, additional findings were observed as well. First, despite tracer delivery using a constant-pressure system, pulsatile flow was observed in some cases[60, 61]. As discussed for ph-OCT, structural pulsatility had already been shown and suspected to be cardiac in nature[22, 23]. While aqueous angiography was not done simultaneously to recording cardiovascular data, aqueous angiography pulsation rates in short video segments were similar to published average non-human primate heart rates[60].

In addition to pulsatile AHO, a novel finding of dynamic AHO was seen (Fig. 6). Suspected by some to be a static set of fluid pathways, AHO showed the ability to arise in regions without initial signal as well as diminish in regions with initial signal, both in non-human primates and humans[60, 61]. Currently, the mechanism regulating this dynamic change is unclear. Locally, distal AHO pathways are known to have muscular walls such as blood vessels and may have the capability to locally contract (Tan J et al. 2017; ARVO Paper 3771). Alternatively, local TM regulation could also be at play. Either way, dynamic AHO was a unique finding that may allow for discovery of new points of outflow regulation. Dynamic change where a region could develop new angiographic signal was also consistent with the observations that low flow regions could be rescued by trabecular bypass[59]. Therefore, it may be that low flow regions are not permanently so and that AHO can be established with proper surgical maneuvers or disease treatment.

While showing segmental AHO that was similar to other static and real-time methods, aqueous angiography has limitations as well. Tracer delivery into the AC, while allowing for more simultaneous and circumferential delivery to TM/SC, wasn't fully physiologic. Aqueous normally enters the eye posterior to the iris, and tracer delivery anterior to the iris (in the AC) can cause artificial deepening of the chamber. Confounders related to post-mortem eye studies also existed such as lost cellular viability and clotting of episcleral veins. Use of lid speculum in imaging of live non-human primates[60] and humans[61] may have altered ocular surface pressure. Additionally, non-human primates required tractions sutures to move the eye which may have created non-physiologic force vectors during eye rotation[60]. Fortunately, in live humans this was not necessary as patients could move their own eyes to command. However, in live humans undergoing cataract surgery, anti-muscarinic dilation drops were also used and likely altered TM capacitance with potential angiographic consequence as well[61].

Nevertheless, many confounders were carefully considered and sometimes carried forth because of clinical realities and practicalities associated with doing research in live subjects. While sulcus delivery of a tracer is more physiologic, no surgeon would place an infusion line in the sulcus of a phakic subject for fear of devastating visual consequences such as phacoanaphylaxis, lens particle glaucoma, vitreous hemorrhages, and hyphemas. Currently, aqueous angiography is most safely done in the operating room so lid speculae and traction sutures are simply unavoidable in non-human primates. Dilation for humans was necessary because it made more sense to first study aqueous angiography concurrent to cataract surgery because patients were already in the operating room for routine surgical care. Additionally, aqueous angiography tracers (fluorescein and ICG) have been described as capsular dyes by the American Academy of Ophthalmology which can facilitate the capsulorhexis[66]. Regarding the AC maintainer itself, after removal, its entry wound was converted into the second instrument side-port for phacocemulsification. In this way, aqueous angiography in live patients required no additional wounds beyond those of normal cataract surgery[61].

In the future, aqueous angiography will be directed at comparing normal and glaucomatous eyes. This can be done with human subjects or glaucoma animal models (cat, dog, or rodent)[67]. The former is more clinically relevant, but careful attention will be required to

exclude patients with low-pressure glaucoma. Without drug holidays, maximum IOPs are not always known for all glaucoma patient. The latter animal experiments are more controlled given precise genetic deletions in the setting of typically identical genetic backgrounds for comparing controls and mutants.

In summary, multiple methods exist for functional conventional (trabecular) AHO assessment. For segmental AHO, there was overall agreement between different labs, using different methods (static vs real-time), in different species (mouse, pig, cow, non-human primate, and human), with different models (post-mortem eyes vs. anterior segment organ culture vs. intact eyes of live subjects), with different tracers. This was all very reassuring. Combining concepts from different methods is also useful. Mathematically modeled, the difference between canalograms and aqueous angiography approximately equals TM function (canalograms – aqueous angiography = TM). Therefore, to segregate proximal (TM) from distal (post-TM) AHO contributions, canalograms and aqueous angiography could be done in the same eye and compared with differences specifically revealing TM AHO contributions.

The use of different tracers also deserves additional comment. As mentioned above, water has a molecular weight of 18 g/mol or daltons. Fluorescein has a molecular weight of ~332 g/mol or daltons and best models water among the tracers published. ICG has a molecular weight of 775 g/mol or daltons and is notably protein bound. This enhances intraluminal retention well-known to be advantageous in choroidal angiography[68]. Therefore, ICG best models protein flow. Beads likely have molecular weight ~10^3–10^7 daltons (consider the number of carbon molecules in a bead) and thus best models larger (particulate-matter) flow in the eye that is reflective of organelle, debris, or cellular (like red blood cell [RBC]) movement. Since aqueous is a complex solution that is more than just water, similar segmental AHO findings despite varying tracer characteristics strongly supports the notion of segmental AHO.

Potential for Non-Invasive Functional Imaging

While aqueous angiography is a new and exciting tool to image AHO, it is invasive. Non-invasive imaging carries both less risk and can be done in the clinic prior to planned surgery. AS-OCT, as mentioned above, fulfills both of these criteria but only images structural parameters of outflow pathways as opposed to the flow itself. In the posterior pole of the eye, OCT angiography (OCTA)[69] is a new modality that images fluid flow, in this case blood in blood vessels. In OCTA, sequential OCTs are acquired close in time at the same location to demonstrate differential intraluminal reflectance due to RBC movement. Using this reflectance-based motion-data, OCTA can image RBC movement which is representative of blood flow. Clinically, early posterior segment OCTA research has shown differences in various vascular retinopathies and changes in response to treatment[70]. Differences have also been reported in glaucomatous compared to normal microvasculature at both the optic nerve head[71] and macula[72].

Given the commercial availability of posterior segment OCTA and the explosion of retinal OCTA research, discussion of OCTA for anterior segment AHO is warranted. This is

particularly so given that OCTA and aqueous angiography are sometimes confused. Unfortunately, anterior segment OCTA is both currently commercially unavailable and not likely to be useful for AHO study. Since OCTA requires particulate motion, the normally clear aqueous humor has no inherent RBC-like material that gives OCT reflectance that can then be varied on sequential scans. Efforts to create OCT contrast agents are underway and can include gold particles[73], milk, or even carriers of commercially available drugs (such as in propofol) (van Oterendorp et al. 2016; ARVO Poster A0111). However, all of these still require tracer introduction into the eye, and at that point these methods become just as invasive as aqueous angiography.

Therefore, for true non-invasive imaging, one needs to identify a native aqueous humor candidate that is present at much higher levels in the aqueous humor compared to the serum. In this way, AHO can be distinguished from ocular surface blood flow. At present, one potential candidate is vitamin C. Found at nearly 100 times increased levels in the aqueous compared to serum[74], vitamin C has been hypothesized to play a role in cornea health. Unfortunately, as a chemically bland molecule, native vitamin C autofluorescence places it in an ultraviolet range not amenable to common clinical imaging. Clever solutions such as chemically attaching vitamin C to a fluorescent molecule followed by oral ingestion and total body loading could be considered.

Conclusion

Structurally, OCT *can* identify outflow lumens. However, there are challenges like the difficulty of acquiring such a large number of high quality images to comprehensively map AHO structure around the limbus. Also, since automated segmentation software searches for low reflectance lumens, simultaneously non-AHO and low-reflectance luminal structures like arteries, lymphatics, or some veins can be confused for AHO pathways. This is unlike the posterior segment where blood vessels are the only luminal structure so that all lumens are related to the movement of only one fluid, blood. Furthermore, unlike the posterior segment, current OCTA methods will unlikely be useful for AHO imaging given the lack of an AC particle that can be differentially identified on sequential scans.

For functional imaging, aqueous angiography now represents a new tool for AHO assessment. Using aqueous angiography, investigators can study differences between normal and glaucomatous eyes. Aqueous angiography data may help identify new pharmacologic therapeutics by demonstrating increased homogenization of initially segmental flow. Surgically, aqueous angiography may help guide trabecular-targeted MIGS for better IOP lowering results. Unfortunately, a limitation is that aqueous angiography is invasive and currently only available in the operating room. Similar to how retinal intravenous fluorescein angiography was initially a cumbersome method, time and evolution will need to occur to stream-line aqueous angiography as well.

In conclusion, a greater understanding of AHO and the anterior segment will likely arise by combining structural and functional data. In the anterior segment, the precise relationship between structural outflow characteristics and functional measures of flow currently does not exist. Simultaneous AHO structural and functional investigation in the same subject and

eye will likely be critical. Alternatively, new imaging modalities targeting native aqueous humor agents could be developed for non-invasive functional imaging.

Acknowledgments

Grant Support:

Funding for this work came from National Institutes of Health, Bethesda, MD (K08EY024674 [ASH]) American Glaucoma Society (AGS) Young Clinician Scientist Award 2015 [ASH]; Research to Prevent Blindness Career Development Award 2016 [ASH]; and an unrestricted grant from Research to Prevent Blindness (New York, NY).

References

1. Macknight AD, McLaughlin CW, Peart D, et al. Formation of the aqueous humor. Clin Exp Pharmacol Physiol. 2000; 27(1–2):100–6. [PubMed: 10696536]
2. Brubaker RF. Goldmann's equation and clinical measures of aqueous dynamics. Exp Eye Res. 2004; 78(3):633–7. [PubMed: 15106943]
3. Johnson M. What controls aqueous humour outflow resistance? Exp Eye Res. 2006; 82(4):545–57. [PubMed: 16386733]
4. Ascher KW. The Aqueous Veins. In: Ritch R, , Caronia RM, editorsClassic Papers in Glaucoma Netherlands: Kugler Publications; 2000
5. Swaminathan SS, Oh DJ, Kang MH, Rhee DJ. Aqueous outflow: segmental and distal flow. J Cataract Refract Surg. 2014; 40(8):1263–72. [PubMed: 25088623]
6. Sit AJ, Ekdawi NS, Malihi M, McLaren JW. A novel method for computerized measurement of episcleral venous pressure in humans. Exp Eye Res. 2011; 92(6):537–44. [PubMed: 21463627]
7. Bill A. The aqueous humor drainage mechanism in the cynomolgus monkey (Macaca irus) with evidence for unconventional routes. Invest Ophthalmol. 1965; 4(5):911–9. [PubMed: 4157891]
8. Bill A. Effects of atropine and pilocarpine on aqueous humour dynamics in cynomolgus monkeys (Macaca irus). Exp Eye Res. 1967; 6(2):120–5. [PubMed: 4960736]
9. Bill A. Aqueous humor dynamics in monkeys (Macaca irus and Cercopithecus ethiops). Exp Eye Res. 1971; 11(2):195–206. [PubMed: 5001096]
10. SHA, NWR. Structure and Mechanism of Uveoscleral Outflow. In: Francis BA, Sarkisian SR, , Tan JC, editorsMinimally Invasive Glaucoma Surgery New York: Thieme; 2017
11. Yucel YH, Johnston MG, Ly T, et al. Identification of lymphatics in the ciliary body of the human eye: a novel "uveolymphatic" outflow pathway. Exp Eye Res. 2009; 89(5):810–9. [PubMed: 19729007]
12. Ashton N. Anatomical study of Schlemm's canal and aqueous veins by means of neoprene casts. Part I. Aqueous veins. Br J Ophthalmol. 1951; 35(5):291–303. [PubMed: 14830741]
13. Van Buskirk EM. The canine eye: the vessels of aqueous drainage. Invest Ophthalmol Vis Sci. 1979; 18(3):223–30. [PubMed: 422328]
14. Ujiie K, Bill A. The drainage routes for aqueous humor in monkeys as revealed by scanning electron microscopy of corrosion casts. Scan Electron Microsc. 1984; (Pt 2):849–56. [PubMed: 6385223]
15. DVORAK-THEOBALD G. Further studies on the canal of Schlemm; its anastomoses and anatomic relations. Am J Ophthalmol. 1955; 39(4 Pt 2):65–89. [PubMed: 14361607]
16. Hann CR, Bentley MD, Vercnocke A, et al. Imaging the aqueous humor outflow pathway in human eyes by three-dimensional micro-computed tomography (3D micro-CT). Exp Eye Res. 2011; 92(2):104–11. [PubMed: 21187085]
17. Huang D, Swanson EA, Lin CP, et al. Optical coherence tomography. Science. 1991; 254(5035): 1178–81. [PubMed: 1957169]
18. Kagemann L, Wollstein G, Ishikawa H, et al. Identification and assessment of Schlemm's canal by spectral-domain optical coherence tomography. Invest Ophthalmol Vis Sci. 2010; 51(8):4054–9. [PubMed: 20237244]

19. Gold ME, Kansara S, Nagi KS, et al. Age-related changes in trabecular meshwork imaging. Biomed Res Int. 2013; 2013:295204. [PubMed: 24163814]
20. Chen RI, Barbosa DT, Hsu CH, et al. Ethnic differences in trabecular meshwork height by optical coherence tomography. JAMA Ophthalmol. 2015; 133(4):437–41. [PubMed: 25634557]
21. Fernández-Vigo JI, García-Feijóo J, Martínez-de-la-Casa JM, et al. Morphometry of the trabecular meshwork in vivo in a healthy population using fourier-domain optical coherence tomography. Invest Ophthalmol Vis Sci. 2015; 56(3):1782–8. [PubMed: 25698706]
22. Hariri S, Johnstone M, Jiang Y, et al. Platform to investigate aqueous outflow system structure and pressure-dependent motion using high-resolution spectral domain optical coherence tomography. J Biomed Opt. 2014; 19(10):106013. [PubMed: 25349094]
23. Li P, Shen TT, Johnstone M, Wang RK. Pulsatile motion of the trabecular meshwork in healthy human subjects quantified by phase-sensitive optical coherence tomography. Biomed Opt Express. 2013; 4(10):2051–65. [PubMed: 24156063]
24. Spaide RF, Curcio CA. Anatomical correlates to the bands seen in the outer retina by optical coherence tomography: literature review and model. Retina. 2011; 31(8):1609–19. [PubMed: 21844839]
25. Kagemann L, Wollstein G, Ishikawa H, et al. 3D visualization of aqueous humor outflow structures in-situ in humans. Exp Eye Res. 2011; 93(3):308–15. [PubMed: 21514296]
26. Kagemann L, Wollstein G, Ishikawa H, et al. Visualization of the conventional outflow pathway in the living human eye. Ophthalmology. 2012; 119(8):1563–8. [PubMed: 22683063]
27. Li P, Butt A, Chien JL, et al. Characteristics and variations of in vivo Schlemm's canal and collector channel microstructures in enhanced-depth imaging optical coherence tomography. Br J Ophthalmol. 2016
28. Huang AS, Belghith A, Dastiridou A, et al. Automated circumferential construction of first-order aqueous humor outflow pathways using spectral-domain optical coherence tomography. J Biomed Opt. 2017; 22(6):66010. [PubMed: 28617922]
29. Li G, Farsiu S, Chiu SJ, et al. Pilocarpine-induced dilation of Schlemm's canal and prevention of lumen collapse at elevated intraocular pressures in living mice visualized by OCT. Invest Ophthalmol Vis Sci. 2014; 55(6):3737–46. [PubMed: 24595384]
30. Li G, Mukherjee D, Navarro I, et al. Visualization of conventional outflow tissue responses to netarsudil in living mouse eyes. Eur J Pharmacol. 2016; 787:20–31. [PubMed: 27085895]
31. Skaat A, Rosman MS, Chien JL, et al. Microarchitecture of Schlemm Canal Before and After Selective Laser Trabeculoplasty in Enhanced Depth Imaging Optical Coherence Tomography. J Glaucoma. 2017; 26(4):361–6. [PubMed: 28079655]
32. Kagemann L, Wang B, Wollstein G, et al. IOP elevation reduces Schlemm's canal cross-sectional area. Invest Ophthalmol Vis Sci. 2014; 55(3):1805–9. [PubMed: 24526436]
33. Bentley MD, Hann CR, Fautsch MP. Anatomical Variation of Human Collector Channel Orifices. Invest Ophthalmol Vis Sci. 2016; 57(3):1153–9. [PubMed: 26975026]
34. Hann CR, Vercnocke AJ, Bentley MD, et al. Anatomic changes in Schlemm's canal and collector channels in normal and primary open-angle glaucoma eyes using low and high perfusion pressures. Invest Ophthalmol Vis Sci. 2014; 55(9):5834–41. [PubMed: 25139736]
35. Huang AS, Kim LA, Fawzi AA. Clinical characteristics of a large choroideremia pedigree carrying a novel CHM mutation. Arch Ophthalmol. 2012; 130(9):1184–9. [PubMed: 22965595]
36. Tatham AJ, Weinreb RN, Medeiros FA. Strategies for improving early detection of glaucoma: the combined structure-function index. Clin Ophthalmol. 2014; 8:611–21. [PubMed: 24707166]
37. Lisboa R, Weinreb RN, Medeiros FA. Combining structure and function to evaluate glaucomatous progression: implications for the design of clinical trials. Curr Opin Pharmacol. 2013; 13(1):115–22. [PubMed: 23219155]
38. Medeiros FA, Lisboa R, Weinreb RN, et al. A combined index of structure and function for staging glaucomatous damage. Arch Ophthalmol. 2012; 130(9):1107–16. [PubMed: 23130365]
39. Battista SA, Lu Z, Hofmann S, et al. Reduction of the available area for aqueous humor outflow and increase in meshwork herniations into collector channels following acute IOP elevation in bovine eyes. Invest Ophthalmol Vis Sci. 2008; 49(12):5346–52. [PubMed: 18515571]

40. Swaminathan SS, Oh DJ, Kang MH, et al. Secreted protein acidic and rich in cysteine (SPARC)-null mice exhibit more uniform outflow. Invest Ophthalmol Vis Sci. 2013; 54(3):2035–47. [PubMed: 23422826]
41. Sabanay I, Gabelt BT, Tian B, et al. H-7 effects on the structure and fluid conductance of monkey trabecular meshwork. Arch Ophthalmol. 2000; 118(7):955–62. [PubMed: 10900110]
42. Hann CR, Bahler CK, Johnson DH. Cationic ferritin and segmental flow through the trabecular meshwork. Invest Ophthalmol Vis Sci. 2005; 46(1):1–7. [PubMed: 15623746]
43. Ethier CR, Chan DW. Cationic ferritin changes outflow facility in human eyes whereas anionic ferritin does not. Invest Ophthalmol Vis Sci. 2001; 42(8):1795–802. [PubMed: 11431444]
44. Lu Z, Overby DR, Scott PA, et al. The mechanism of increasing outflow facility by rho-kinase inhibition with Y-27632 in bovine eyes. Exp Eye Res. 2008; 86(2):271–81. [PubMed: 18155193]
45. Braakman ST, Read AT, Chan DW, et al. Colocalization of outflow segmentation and pores along the inner wall of Schlemm's canal. Exp Eye Res. 2015; 130:87–96. [PubMed: 25450060]
46. Vranka JA, Bradley JM, Yang YF, et al. Mapping molecular differences and extracellular matrix gene expression in segmental outflow pathways of the human ocular trabecular meshwork. PLoS One. 2015; 10(3):e0122483. [PubMed: 25826404]
47. Keller KE, Bradley JM, Vranka JA, Acott TS. Segmental versican expression in the trabecular meshwork and involvement in outflow facility. Invest Ophthalmol Vis Sci. 2011; 52(8):5049–57. [PubMed: 21596823]
48. Ren R, Li G, Le TD, et al. Netarsudil Increases Outflow Facility in Human Eyes Through Multiple Mechanisms. Invest Ophthalmol Vis Sci. 2016; 57(14):6197–209. [PubMed: 27842161]
49. Zhu JY, Ye W, Gong HY. Development of a novel two color tracer perfusion technique for the hydrodynamic study of aqueous outflow in bovine eyes. Chin Med J (Engl). 2010; 123(5):599–605. [PubMed: 20367989]
50. Fellman RL, Grover DS. Episcleral venous fluid wave: intraoperative evidence for patency of the conventional outflow system. J Glaucoma. 2014; 23(6):347–50. [PubMed: 23282859]
51. Fellman RL, Feuer WJ, Grover DS. Episcleral Venous Fluid Wave Correlates with Trabectome Outcomes: Intraoperative Evaluation of the Trabecular Outflow Pathway. Ophthalmology. 2015; 122(12):2385–91e1. [PubMed: 26477844]
52. Aktas Z, Tian B, McDonald J, et al. Application of canaloplasty in glaucoma gene therapy: where are we? J Ocul Pharmacol Ther. 2014; 30(2–3):277–82. [PubMed: 24512297]
53. Grieshaber MC. Ab externo Schlemm's canal surgery: viscocanalostomy and canaloplasty. Dev Ophthalmol. 2012; 50:109–24. [PubMed: 22517178]
54. Grieshaber MC, Pienaar A, Olivier J, Stegmann R. Clinical evaluation of the aqueous outflow system in primary open-angle glaucoma for canaloplasty. Invest Ophthalmol Vis Sci. 2010; 51(3): 1498–504. [PubMed: 19933180]
55. Zeppa L, Ambrosone L, Guerra G, et al. Using canalography to visualize the in vivo aqueous humor outflow conventional pathway in humans. JAMA Ophthalmol. 2014; 132(11):1281. [PubMed: 25188749]
56. Saraswathy S, Tan JC, Yu F, et al. Aqueous Angiography: Real-Time and Physiologic Aqueous Humor Outflow Imaging. PLoS One. 2016; 11(1):e0147176. [PubMed: 26807586]
57. Huang AS, Mohindroo C, Weinreb RN. Aqueous Humor Outflow Structure and Function Imaging At the Bench and Bedside: A Review. J Clin Exp Ophthalmol. 2016; 7(4)
58. Huang AS, Saraswathy S, Dastiridou A, et al. Aqueous Angiography with Fluorescein and Indocyanine Green in Bovine Eyes. Transl Vis Sci Technol. 2016; 5(6):5.
59. Huang AS, Saraswathy S, Dastiridou A, et al. Aqueous Angiography-Mediated Guidance of Trabecular Bypass Improves Angiographic Outflow in Human Enucleated Eyes. Invest Ophthalmol Vis Sci. 2016; 57(11):4558–65. [PubMed: 27588614]
60. Huang AS, Li M, Yang D, et al. Aqueous Angiography in Living Nonhuman Primates Shows Segmental, Pulsatile, and Dynamic Angiographic Aqueous Humor Outflow. Ophthalmology. 2017
61. Huang AS, Camp A, Xu BY, et al. Aqueous Angiography: Aqueous Humor Outflow Imaging in Live Human Subjects. Ophthalmology. 2017

62. Craven ER, Katz LJ, Wells JM, Giamporcaro JE. Cataract surgery with trabecular micro-bypass stent implantation in patients with mild-to-moderate open-angle glaucoma and cataract: two-year follow-up. J Cataract Refract Surg. 2012; 38(8):1339–45. [PubMed: 22814041]

63. Minckler D, Mosaed S, Dustin L, Ms BF. Trabectome (trabeculectomy-internal approach): additional experience and extended follow-up. Trans Am Ophthalmol Soc. 2008; 106:149–59. discussion 59–60. [PubMed: 19277230]

64. Johnstone M, , Jamil A, , Martin E. Aqueous Veins and Open Angle Glaucoma. In: Schacknow PN, , Samples JR, editorsThe Glaucoma Book: A Practical, Evidence-Based Approach to Patient Care New York: Springer; 2010

65. Parikh HA, Loewen RT, Roy P, et al. Differential Canalograms Detect Outflow Changes from Trabecular Micro-Bypass Stents and Ab Interno Trabeculectomy. Sci Rep. 2016; 6:34705. [PubMed: 27811973]

66. Jacobs DS, Cox TA, Wagoner MD, et al. Capsule staining as an adjunct to cataract surgery: a report from the American Academy of Ophthalmology. Ophthalmology. 2006; 113(4):707–13. [PubMed: 16581432]

67. Kuehn MH, Lipsett KA, Menotti-Raymond M, et al. A Mutation in LTBP2 Causes Congenital Glaucoma in Domestic Cats (Felis catus). PLoS One. 2016; 11(5):e0154412. [PubMed: 27149523]

68. Keane PA, Sadda SR. Imaging chorioretinal vascular disease. Eye (Lond). 2010; 24(3):422–7. [PubMed: 20010789]

69. Gao SS, Jia Y, Zhang M, et al. Optical Coherence Tomography Angiography. Invest Ophthalmol Vis Sci. 2016; 57(9):OCT27–36. [PubMed: 27409483]

70. Ghasemi Falavarjani K, Iafe NA, Hubschman JP, et al. Optical Coherence Tomography Angiography Analysis of the Foveal Avascular Zone and Macular Vessel Density After Anti-VEGF Therapy in Eyes With Diabetic Macular Edema and Retinal Vein Occlusion. Invest Ophthalmol Vis Sci. 2017; 58(1):30–4. [PubMed: 28114569]

71. Akil H, Huang AS, Francis BA, et al. Retinal vessel density from optical coherence tomography angiography to differentiate early glaucoma, pre-perimetric glaucoma and normal eyes. PLoS One. 2017; 12(2):e0170476. [PubMed: 28152070]

72. Yarmohammadi A, Zangwill LM, Diniz-Filho A, et al. Peripapillary and Macular Vessel Density in Patients with Glaucoma and Single-Hemifield Visual Field Defect. Ophthalmology. 2017; 124(5): 709–19. [PubMed: 28196732]

73. Wang B, Kagemann L, Schuman JS, et al. Gold nanorods as a contrast agent for Doppler optical coherence tomography. PLoS One. 2014; 9(3):e90690. [PubMed: 24595044]

74. PURCELL EF, LERNER LH, KINSEY VE. Ascorbic acid in aqueous humor and serum of patients with and without cataract; physiologic significance of relative concentrations. AMA Arch Ophthalmol. 1954; 51(1):1–6. [PubMed: 13103879]

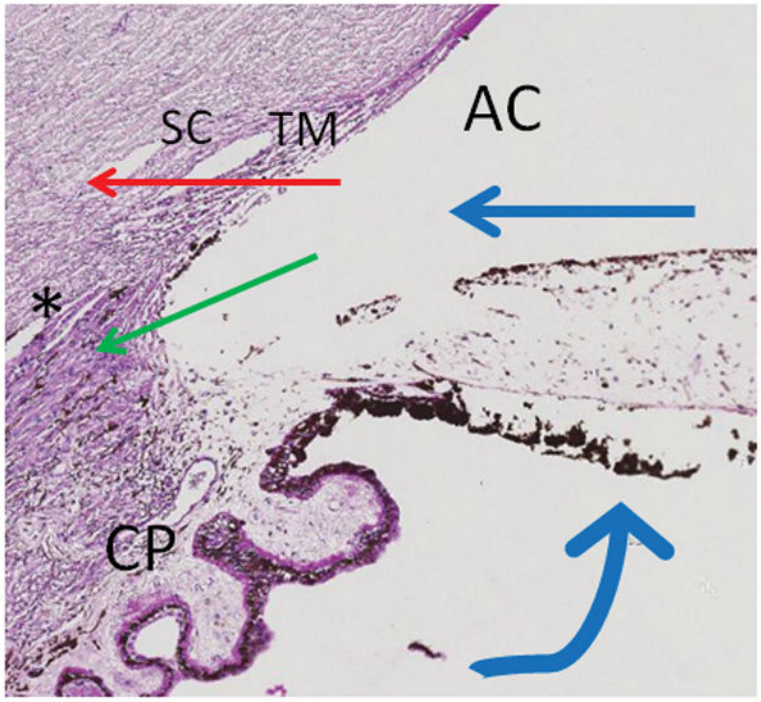

Figure 1. Aqueous Humor Outflow (AHO)

Aqueous humor is produced at ciliary processes (CP) and flows from the sulcus space into the anterior chamber (AC). At that point, there are two outflow pathways. The conventional (trabecular) pathway (red arrow) moves past the trabecular meshwork (TM) into Schlemm's Canal (SC) ultimately leading to venous system and the right side of the heart. The unconventional (uveoscleral) pathway (green arrow) enters into the ciliary body band at the angle into ciliary body clefts (asterisk).

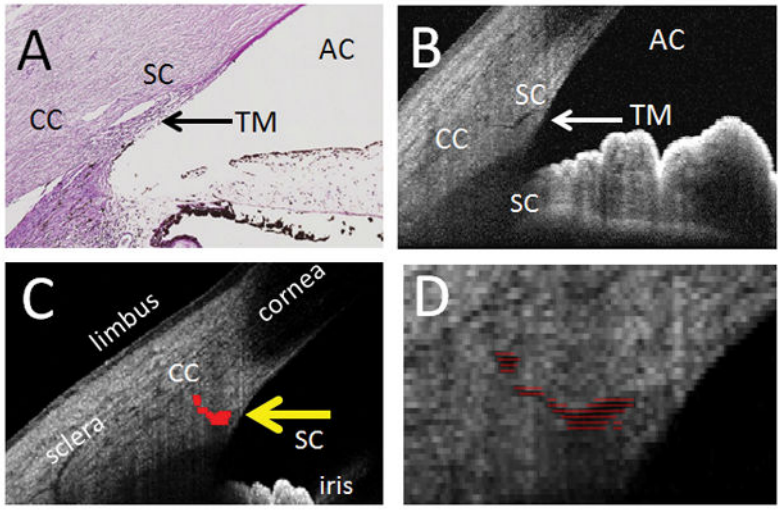

Figure 2. AHO Assessment by OCT and Automated Segmentation

A) Histological anatomy of the human anterior segment angle (PAS stain) showing the anterior chamber (AC), trabecular meshwork (TM), Schlemm's Canal (SC), and a collector channel (CC). B) OCT B-scan of the human anterior segment angle with similar structures seen. C) Automated segmentation of SC (yellow arrow) and first order CC. D) Expanded view of the segmentation from panel C.

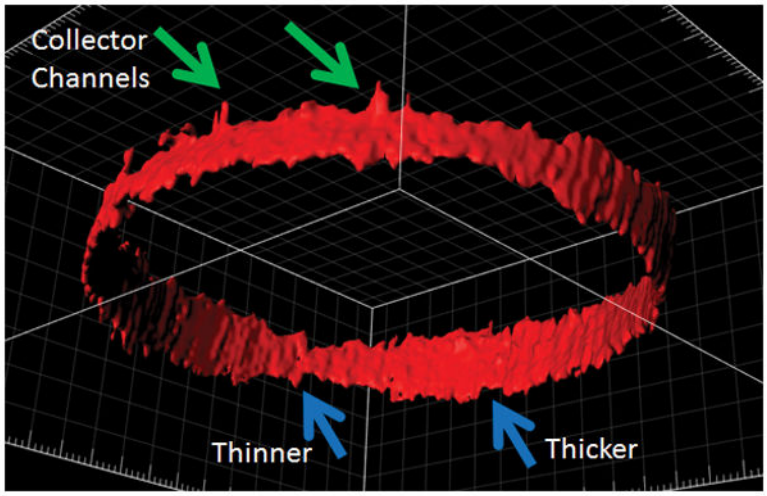

Figure 3. Circumferential (360-degree) Reconstruction of Live Human Outflow Pathways

Anterior-segment OCT was performed circumferential around the limbus of the right eye of a healthy male. A three-dimensional AHO cast was created based on automated segmentation of Schlemm's Canal (SC; blue arrows) and first order collector channels (green arrows). Areas of thicker and thinner SC are seen.

Figure 4. Heidelberg Engineering FLEX Module

The FLEX module is a fully-functional Spectralis HRA+OCT that is installed on a modified surgical boom arm as opposed to a table top. A 500-pound base provides stability. Multiple pivot joints allow imaging in nearly any body position. A micromanipulator (yellow arrow) allows for precise z-axis adjustments. Initial unmodified image provided courtesy of Heidelberg Engineering.

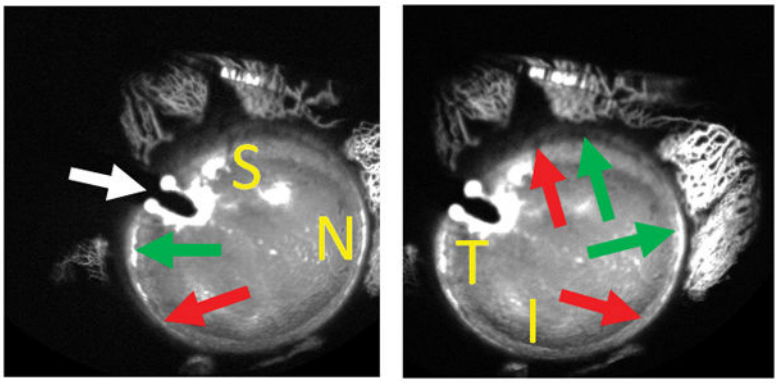

Figure 5. Aqueous Angiography During Cataract Surgery

Aqueous angiography was performed in the right eye of a 73-year-old female during cataract surgery with 2% fluorescein diluted in balanced salt solution. The anterior chamber maintainer entered superior-temporal (white arrow) to allow space inferior-temporal for placement of an eventual phacoemulsification main wound. The subject moved her eye slightly to the right (A) and left (B) to allow viewing of different regions (S = superior, N = nasal, T = temporal, and I = inferior). Peri-limbal, there were segmental regions with (green arrows) and without (red arrow) angiographic aqueous humor outflow.

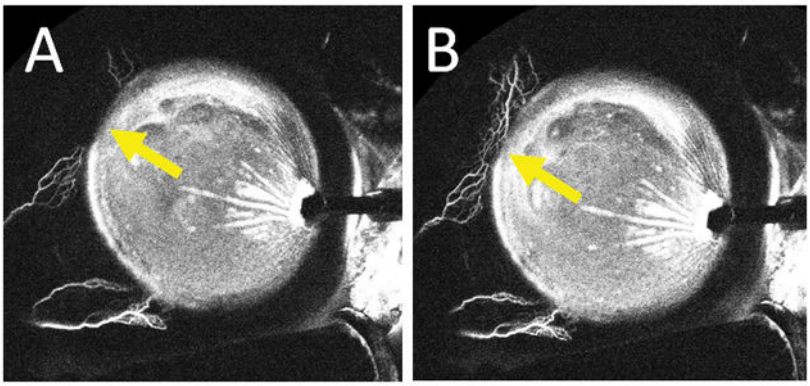

Figure 6. Dynamic Angiographic Aqueous Humor Outflow Seen by Aqueous Angiography

Aqueous angiography was performed in the left eye of a 61-year-old female during cataract surgery with 0.4% indocyanine green diluted in balanced salt solution. The right side of the images is temporal and the left side is nasal. The anterior chamber maintainer inserted into the eye temporally. A) 176 seconds after tracer introduction and B) 182 seconds after tracer introduction. Yellow arrows show increasing angiographic signal superior-nasal over 6 seconds.